ACS APPLIED MATERIALS & INTERFACES

Research Article

www.acsami.org

Electric Field Cycling Behavior of Ferroelectric Hafnium Oxide

Tony Schenk,*[,†] Uwe Schroeder,[†] Milan Pešić,[†] Mihaela Popovici,[‡] Yuriy V. Pershin,[§] and Thomas Mikolajick[†,∥]

[†]NaMLab gGmbH, Noethnitzer Str. 64, D-01187 Dresden, Germany

[‡]Imec, Kapeldreef 75, B-3001 Leuven, Belgium

[§]Department of Physics and Astronomy, and the University of South Carolina Nanocenter, University of South Carolina, Columbia, South Carolina 29208, United States

[∥]Chair of Nanoelectronic Materials, TU Dresden, D-01062 Dresden, Germany

Supporting Information

ABSTRACT: HfO_2 based ferroelectrics are lead-free, simple binary oxides with nonperovskite structure and low permittivity. They just recently started attracting attention of theoretical groups in the fields of ferroelectric memories and electrostatic supercapacitors. A modified approach of harmonic analysis is introduced for temperature-dependent studies of the field cycling behavior and the underlying defect mechanisms. Activation energies for wake-up and fatigue are extracted. Notably, all values are about 100 meV, which is 1 order of magnitude lower than for conventional ferroelectrics like lead zirconate titanate (PZT). This difference is mainly atttributed to the one to two orders of magnitude higher electric fields used for cycling and to the different surface to volume ratios between the 10 nm thin films in this study and the bulk samples of former measurements or simulations. Moreover, a new, analog-like split-up effect of switching peaks by field cycling is discovered and is explained by a network model based on memcapacitive behavior as a result of defect redistribution.

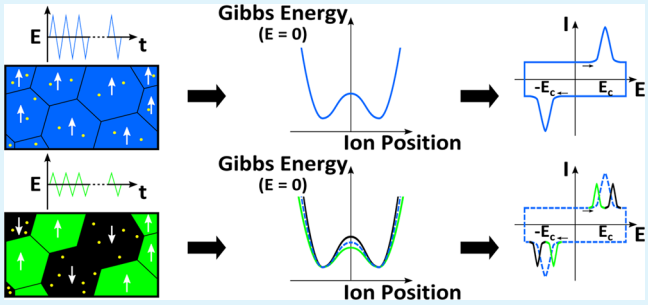

KEYWORDS: *hafnium oxide, ferroelectrics, harmonic analysis, fatigue, wake-up, field cycling behavior*

INTRODUCTION

Hafnium oxide was recently reported to exhibit ferroelectric behavior.[1] From the material point of view, HfO_2 based ferroelectrics are of special interest because they are lead-free, simple binary oxides and exhibit a nonperovskite structure with a comparably low relative permittivity in the range of ∼20−30.[1] Thus, first simulation efforts with focus on ferroelectricity in HfO_2 were started.[2,3] Moreover, a recent simulation-based material design search indicated that there are further (anti-) ferroelectric compounds to be discovered[4] and motivated a theoretical work on antiferroelectricity in the chemically very similar ZrO_2.[5] Nonetheless, this marks just a starting point. Many questions concerning the tuning of the ferroelectric properties and the role of defects are studied far less extensively than, for example, for lead zirconate titanate (PZT). Thus, the transfer of promising analysis methods is the first step for deepening the understanding of this material system. From the application point of view, HfO_2 based ferroelectrics attracted attention especially in the field of ferroelectric memories[1,6,7] and recently also for electrostatic supercapacitors.[8] Since 2007, HfO_2 is the state-of-the-art gate dielectric in complementary metal-oxide-semiconductor technology[10] and, therefore, is also a promising candidate to overcome integration and scaling issues associated with conventional ferroelectrics.[11] Ferroelectric field effect transistors in 28 nm technology[12] evidenced this potential already in 2012.

RESULTS AND DISCUSSION

The present work is dedicated to the field cycling behavior of Sr:HfO_2, which showed ferroelectric hystereses with remanent polarizations up to 23 $\mu C/cm^2$ and the highest coercive fields (∼2 MV/cm) of all tested dopants so far.[13] Also, the conditioning behavior of a pristine sample (wake-up) was shown: Two distinct current peaks merge during cycling causing a constricted polarization hysteresis to become more ideal and open. Such constricted hystereses were shown by Carl and Hardtl[14] for doped PZT and were attributed to internal bias fields. These fields were assumed to result from incorporated defects, which either pin domains walls or form anisotropic centers favoring one direction of the spontaneous polarization.[14] Further possible roots for constrictions and deformations of hystereses are reviewed elsewhere.[15]

This paper is focused on the following:

Received: July 22, 2014
Accepted: November 3, 2014
Published: November 3, 2014

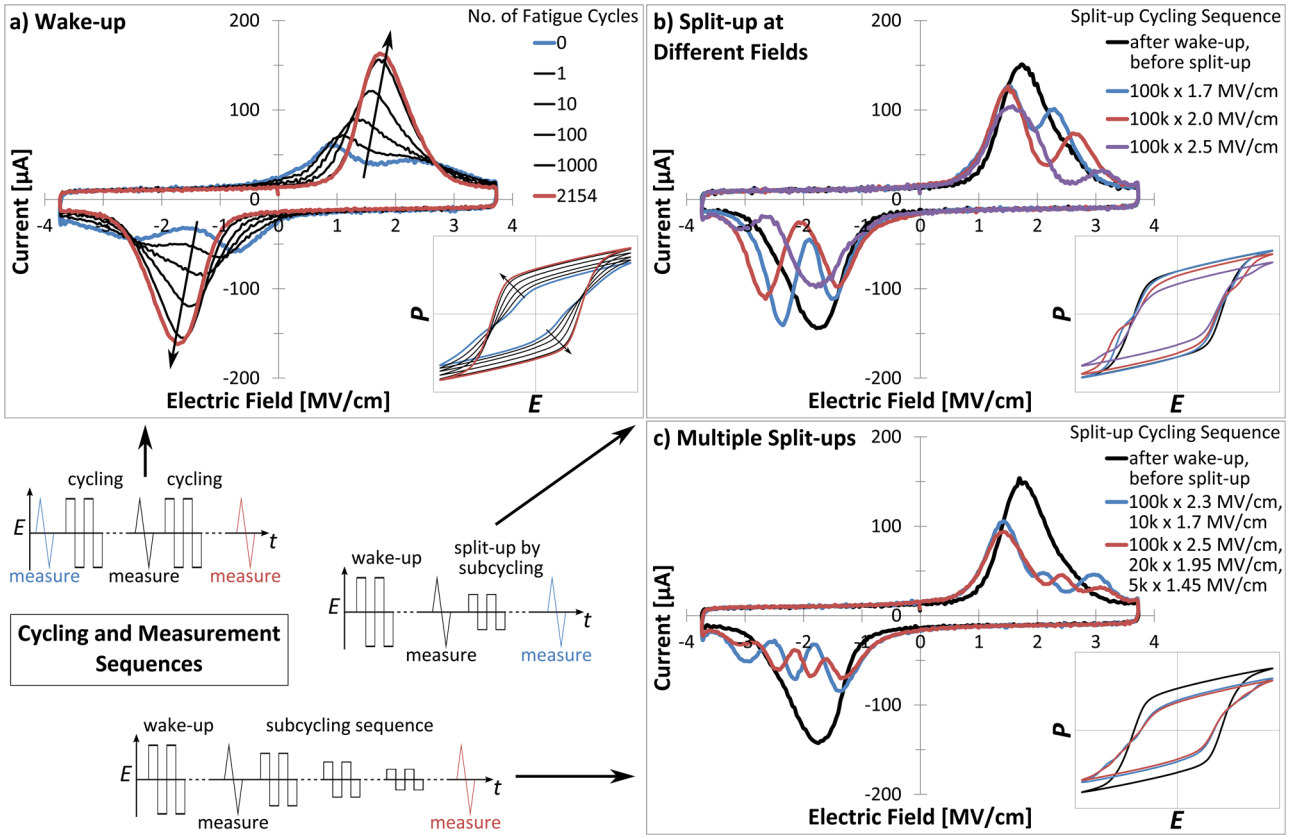

Figure 1. (a) Wake-up effect: The constricted hysteresis of a pristine sample opens after field cycling and two distinct current peaks merge into one single peak. (b) Current peak split-ups occur directly at the values of the cycling field amplitude (constant no. of cycles). (c) Split-up of multiple peaks by subsequent field cycling with different field amplitudes in descending order. The split-up at 1.45 MV/cm has already vanished in the first quadrant (red line). All experiments were performed with $f = 1000$ Hz. The corresponding P–E hystereses are shown as insets with the E- and P-axes scaled from −4 MV/cm to 4 MV/cm and from −30 μC/cm^2 to 30 μC/cm^2, respectively.

(1) A new analog split-up phenomenon of ferroelectric switching peaks in the transient current response which was modeled as a result of defect redistribution.
(2) Up to now, the first temperature dependent measurements to determine activation energies for the three defect related effects wake-up, fatigue, and the aforementioned split-up phenomenon. A new convenient and time saving approach of harmonic analysis was introduced for this purpose.

Wake-up refers to the conditioning effect of a pristine sample, as it was reported also for Y[16] or Si doped HfO_2[12,17,18] and for PZT:[19] The pinched hysteresis of a pristine sample opens as the electric field is progressively cycled up and down. In the observed current response, this is reflected in the merging of two or more distinct current maxima into one single peak on each side of the electric field, as can be seen from Figure 1a.

By applying an electric field that cycles the ferroelectric in a subloop of the former wake-up procedure, an increasingly constricted hysteresis can be observed. The corresponding curves of the current I versus the electric field E, then, show a progressing peak split-up right at the voltage of the cycling field (see Figure 1b). The more subcycles that are applied, the more pronounced the split-up in the I–E and the constriction in the P–E graph become (see Figure S1 of the Supporting Information). The procedure of remerging the peaks by the cycling with the original, high-field amplitude of 3.75 MV/cm shows a clear trend: The higher the subcycling amplitude, the more cycles that are required to both split-up the corresponding two peaks during subcycling and remerge them later again with 3.75 MV/cm amplitude.

As mentioned before, constricted hystereses and their depinching by a higher field amplitude were reported earlier also for PZT. However, to the authors' knowledge, a pinching by field cycling with lower amplitude has not been reported yet. In addition to this new observation, the split-up of multiple peaks is possible as shown in Figure 1c. For this purpose, the desired cycling amplitudes have to be applied in descending order to not remerge previously split-up peaks. This peak split-up appears to be possible in an analogous way and in any arbitrary configuration only depending on the appropriate selection of voltages and their according number of split-up cycles.

In the following, harmonic analysis[20,21] was applied to study this effect and also to study the defect-related phenomena of polarization fatigue and wake-up. Morozov and Damjanovic used a setup with a lock-in amplifier to analyze amplitudes and phases up to the ninth harmonic.[21] They found a phase jump in the third harmonic during the transition from a constricted to an open hysteresis. Exploiting such features that mark a clear point in time makes this method superior to simply arguing with the P–E or I–E curves. Moreover, comparisons to predictions of hystereses models like the Preisach model[22] can be drawn (see Supporting Information S3 and S4). Nonetheless, the method is not limited by the conformity of the hystereses to any model prediction. If a certain feature such as a

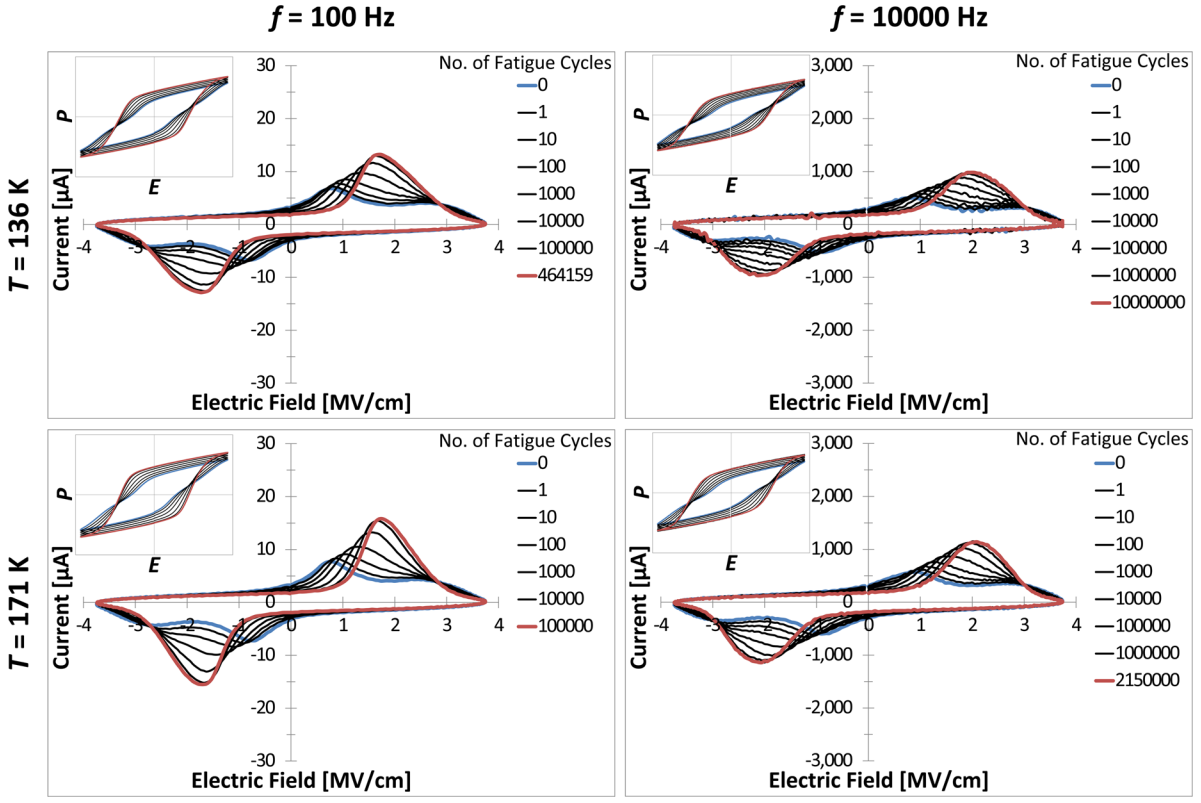

Figure 2. *I*–*E* hystereses for 100 Hz and 10 kHz at 136 and 171 K. The corresponding *P*–*E* hystereses are shown as insets with the *E*- and *P*-axes scaled from −4 MV/cm to 4 MV/cm and from −30 μC/cm^2 to 30 μC/cm^2, respectively.

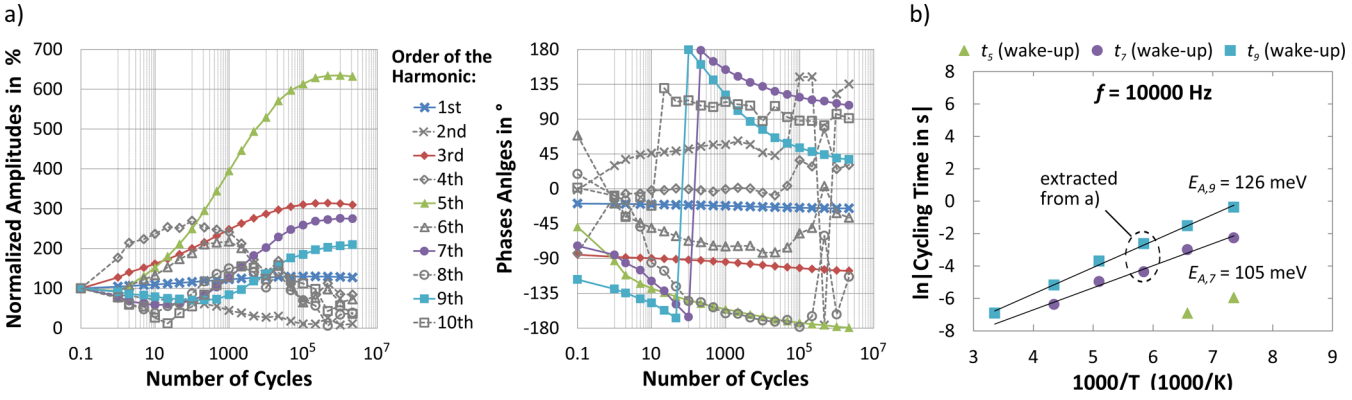

Figure 3. (a) Example of the evolution of amplitude (normalized to the respective initial value) and phase against the number of fatigue cycles for f = 10 000 Hz and T = 171 K. Jumps in the phase of the seventh and ninth harmonics occur subsequently and are accompanied by a minimum in the amplitude. (b) Arrhenius-plot of the cycling time at which the phase jumps of the respective harmonic was observed for f = 10 000 Hz. Data points were extracted from (a) as shown and similarly for the other temperatures between 136 and 298 K.

phase jump can be related to the change in the hysteresis shape, it can be used to mark a clear point in time for the transition from, for example, constricted to nonconstricted. Measurements with different frequencies allow distinguishing whether the cycling time or the number of switching processes is the figure of interest for the underlying mechanism.

However, this lock-in technique suffers one major drawback: A certain number of input-channels is needed to monitor all harmonics at one stretch. Measuring only one harmonic at a time multiplies the measurement time tremendously. Moreover, no *P*–*E* or *I*–*E* curves are obtained. The alternative presented in this work is based on a commercial test system for ferroelectrics and its fatigue measurement environment. It allows automatically acquiring as much dynamic hysteresis measurements (*P*–*E* and *I*–*E* curves) per 10 field cycles as regarded necessary. Afterward, the measured hystereses are subjected to a Fourier series expansion to calculate the corresponding amplitude and phase values:

$$P(t) = P_0 + P_1 \cdot \sin(\omega t + \varphi_1) + P_2 \cdot \sin(\omega t + \varphi_2) + \ldots \quad (1)$$

where P_k represents the amplitude and φ_k represents the phase of the kth harmonic.

This convenient approach is now applied to study, first, the wake-up effect and, later, the fatigue and the split-up phenomenon described at the beginning. The wake-up process slows down as the temperature T is decreased as shown

dx.doi.org/10.1021/am504837r | ACS Appl. Mater. Interfaces 2014, 6, 19744−19751

Table 1. Comparison of Activation Energies for Wake-up, Fatigue, and Remerging after Split-Up

phenomenon[a]	f = 100 Hz	f = 1000 Hz	f = 10 000 Hz
wake-up: $E_{A,7}/E_{A,9}$ in meV	84(±6)/88(±7)	98(±20)/99(±24)	105(±12)/126(±22)
fatigue: E_A in meV	48(±7)	56(±14)	103(±13)
remerging after split-up at 1.9 V: $E_{A,7}/E_{A,9}$ in meV	118(±38)/132(±13)	142(±117)/152(±37)	165(±37)/185(±26)
remerging after split-up at 2.3 V: $E_{A,7}/E_{A,9}$ in meV	105(±29)/129(±22)	111(±40)/129(±28)	124(±28)/138(±35)

[a] $E_{A,7}$ and $E_{A,9}$ are the activation energies for the seventh and ninth harmonics, respectively. For fatigue, only one value is given because the maximum in P_r was used as the criterion.

exemplarily in Figure 2. At 171 K and 10 kHz, about 100 cycles were necessary to no longer see two switching peaks (i.e., a pronounced kink around the coercive field), whereas at 136 K, it took about 1000 cycles. It can be seen that it is difficult to assess the exact point where the two peaks are merged into one peak. As mentioned before, the harmonic analysis provides a potentially more precise quantitative study of the T-dependence. Moreover, additional features are observed: The switching peaks become broader for lower temperatures or higher frequencies and the remanent and maximum polarization decreases with increasing frequency. This indicates that the maximum voltage used here was not high enough to sufficiently saturate all hystereses. Dielectric breakdown limited the applicable electric fields.

Figure 3a exemplarily shows the evolution of amplitude and phase of the first 10 harmonics against the number of fatigue cycles cycling time for 10 kHz at 171 K. A phase jump and an accompanying minimum in amplitude can be seen for the seventh and ninth harmonic. The times of the phase jumps were extracted for all temperatures and are plotted into the Arrhenius-plot in Figure 3b. Activation energies E_A of 105 and 126 meV were extracted for seventh and ninth harmonic, respectively. Because the harmonics are only a mathematical representation of the hysteresis shape, the difference might be surprising, but it is consistent also for all further observations in this work. This could be interpreted as follows: From Figure 3, it can be seen that phase jumps of higher harmonics occurred later in time. Thus, different activation energies could be explained by different mechanisms dominating the hysteresis change at the beginning and at the end of the wake-up process. Moreover, a clear frequency dependence is observed, which can, at least partially, be attributed to the frequency dependent change in the switching characteristics as discussed in more detail in section S5 of the Supporting Information. At 1 kHz, only 98 and 99 meV are extracted for seventh and ninth harmonicsλ, respectively. For 100 Hz, the values of 84 and 88 meV are even lower. In contrast to Morozov and Damjanovic,[20,21] no pure time dependence was observed. Thus, also the number of polarization reversals is important. Quite likely, Morozov and Damjanovic saw only a phase jump in the third harmonic since their observation time was too short to see jumps in higher odd harmonics at the temperatures used. There is no particular reason why only the third harmonic should be affected by the pinching/depinching of a hysteresis.[15]

The effect of polarization fatigue, as it was formerly shown for Sr:HfO_2 in ref 13, was studied by plotting the cycling time at which the remanent polarizations reached its maximum in an Arrhenius plot (Figure S5 of the Supporting Information). Activation energies of 103, 56, and 48 meV were extracted for 10 kHz, 1 kHz, and 100 Hz, respectively. Besides the lower absolute values of E_A, the more pronounced frequency dependence gives rise to the assumption that different mechanisms are responsible/dominant for fatigue and wake-up (compare section S6 of the Supporting Information).

The novel subcycling induced split-up effect or more precisely the remerging after split-up was studied analogously to the wake-up effect by harmonic analysis. First, the samples were subjected to a treatment consisting of 10^3 cycles of 3.75 MV/cm amplitude to ensure a proper wake-up and 10^5 subcycles to induce a split-up into two distinct current peaks. Independent of the frequency used for merging, 1 kHz was used for this pretreatment. To prevent an imprint,[23] a depolarization sequence consisting of 10 cycles with linearly decreasing amplitude from 3.75 MV/cm to 0 MV/cm was applied. Afterward, the samples were cooled down to study the merging during cycling with 3.75 MV/cm at different temperatures again ranging from 298 to 136 K. Similar to Figure 3, the cycling time necessary to remerge the peak completely increases as the temperature decreases (see Figures S6 and S8 of the Supporting Information). The corresponding Arrhenius plots (Figures S7 and S9 of the Supporting Information) reveal activation energies in the range of 100−200 meV, which is slightly higher than that for wake-up and fatigue but, again, frequency dependent as shown in Table 1. E_A is expected to be a function of the field amplitude[21] because this amplitude bends the energetic potential and, therefore, the barrier between the opposite stable ion positions. Because of the limitations given by early dielectric breakdown at too high fields and nonsaturated hystereses at too low fields, we only used 3.75 MV/cm as the wake-up/remerging amplitude. However, similar trends could be achieved by varying the split-up phenomenon relative to the fixed remerging amplitude. Here, split-up fields of 1.9 MV/cm and 2.3 MV/cm were used. As already stated with respect to the split-up experiments shown in Figure 1, more cycles are necessary to remerge a split-up induced by a higher subcycling field. As can be seen from Table 1, a higher subcycling amplitude results in a lower frequency dependence and an overall lower activation energy. The former is in total agreement of the findings in ref 21, which reports higher activation energies for higher merging amplitudes, whereas we encounter the same for lower split-up amplitudes. The latter, that is, the changed frequency dependence, supports the assumption of different mechanisms being involved in all of the phenomena studied here. Again, a difference in $I-E$ and $P-E$ characteristics is observed, which might account for the different values observed for different split-up amplitudes and frequencies (see sections S5 and S7 of the Supporting Information).

Compared to the values of around 0.6−1.2 eV obtained for the wake-up effects (aging/deaging) in PZT[14,21,24] or $BaTiO_3$,[25] all activation energies are nearly 1 order of magnitude lower. Also, the temperature range necessary to study the phenomena on a reasonably accessible time scale is different. In these perovskites, the oxygen vacancies are also the defects held responsible for polarization fatigue.[23] HfO_2 (resistive switch-

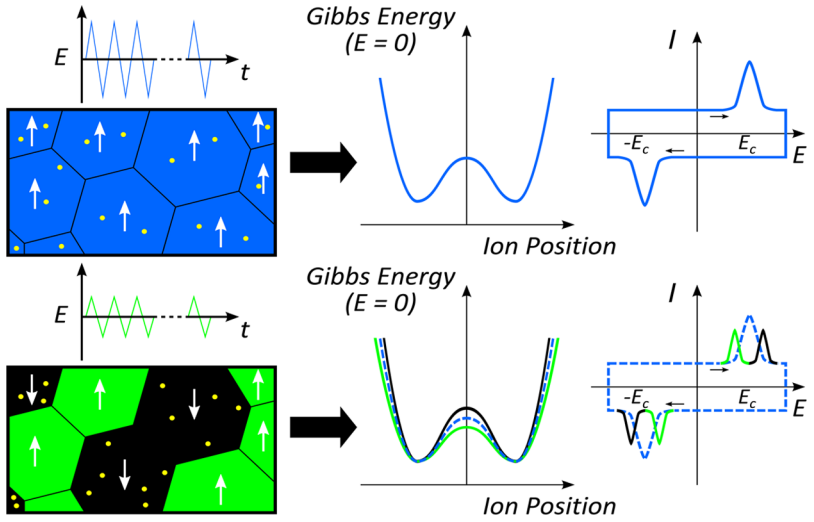

Figure 4. Static domains are assumed to be a preferential place for defect accumulation. Assuming defect related domain wall pinning and seed inhibition mechanism as they are known from ferroelectric fatigue, a progressive inhibition of the nonswitched regions and a facilitated switching of the regions with lower switching fields is concluded. The expected change in Gibbs energy vs ion position and the *I*–*E* curve are sketched on the right.

ing[26]) and the chemically very similar ZrO_2 (fuel cells[27,28]) are known for their high oxygen conductivity.[29,30] Calculated barrier heights for single jumps between distinct positions in the monoclinic lattice can be as low as 50 meV, but overall effective activation energies were calculated to be 0.7 eV for double positively charged O vacancies and even 2.4 eV for neutral ones.[31] The apparent differences to the observations in this work are mainly attributed to the different magnitudes of the applied electric field, several MV/cm for Sr:HfO_2 instead of some 10 kV/cm for PZT. The regime might be altered between the movement and formation of defects within the volume or along domain or grain boundaries. Former studies of Si:HfO_2 revealed that a domain consists of several grains (~30 nm lateral diameter),[32] that is, many domains contain paths that might be preferential for electronic or ionic conduction. In reliability studies on HfO_2 based gate stacks, the activation energies for dielectric breakdown were also reported to increase with higher frequencies[33] similar to what was observed here for fatigue. It is well-known that dielectric breakdown in HfO_2 is related to the generation of oxygen vacancies near the interface layer.[34] In PZT based capacitors, the fatigue issues were also related to a creation of O vacancies. The use of Ir or IrO_2 electrodes solved this problem.[23] Thus, it would not be surprising if future studies revealed a dominant role of oxygen vacancies for the defect-related phenomena of HfO_2 on the basis of ferroelectrics presented here. Although this picture might seem consistent at the present stage of the studies, another possibility to be considered is a (field induced) phase transition. Some examples to assess the order of magnitude are the following: Clima et al.[2] reported values between 230 and 630 meV for the switching barrier between the two opposite polarization states, which depended on the dopant material. Reyes-Lillo et al.[5] calculated a barrier of 35 meV for the transition from tetragonal ($P4_2/nmc$, nonpolar, paraelectric) to the orthorhombic ($Pbc2_1$, polar, ferroelectric) phase in ZrO_2. An upper limit for the transition between the two paraelectric phases of monoclinic ($P2_1/c$, nonpolar) and tetragonal symmetry was simulated to be ~200 meV for both HfO_2 and ZrO_2.[9] However, in the following, only the explanations related to defect movement are considered since they are established for fatigue and wake-up in conventional ferroelectric such as PZT.

To especially explain the analog subcycling dependent split-up phenomenon, a model based on the movement of defects during the switching processes is discussed. The main assumption is static, that is, nonswitching regions are a preferential location for defects to accumulate since such an environment is more stable both from structural and electrical points of view. Figure 4 shows how the Gibbs energy versus (switching) ion position is related to the electric field where the switching current peaks are observed. A higher barrier between the two minima in Gibbs energy results in a higher switching field for the corresponding ion. Whether this accumulation of defects is expected to take place near domain boundaries, electrodes, or within the volume is not specified here. The increasing number of defects progressively impedes the switching of the corresponding domain similar to what is discussed for the mechanisms behind the polarization fatigue: Defects either pin domain walls or inhibit the seeds of domains with opposite polarization near the electrodes.[35] The obtained activation energies are not to be confused with the barrier between two stable states in the Gibbs energy versus ion position shown in the model. The E_A values given here describe the process of defect movement, which is proposed to be the origin of a change in the local switching barriers.

From the broad current peaks in Figure 1, it is clear that the switching field is distributed over a wide field range and lowering the cycling field automatically results in not switching the regions with higher coercive fields any longer. Cycling again with the higher field, these formerly static domains appear as a split-up peak on the higher field side whereas the formerly cycled regions are represented by a peak located below the cycling field. During cycling, the split-up becomes more pronounced. Thus, the switching of the static domains requires higher and higher fields, whereas polarization reversal of the switched regions becomes more and more easy. This is attributed to the distribution of the defects in the film. Hence, this model is able to explain all experimental observation related to the split-up of multiple peaks in any desired configuration as shown in the following. Moreover, it

automatically implies that the situation before the wake-up is a result of a somehow processing related nonuniform defect distribution in addition to a coercive field distribution caused by, for example, different grain sizes that appear after the wake-up.

Given the lack of deeper understanding in the physical mechanism involved in the novel split-up phenomenon, it is helpful to at least proof, if the proposed model is reasonable from a mathematical point of view. According to the above experimental data, Sr:HfO_2 exhibits a capacitive-type response, which depends upon the previous history of voltages applied to this material. In modern parlance,[36] such a system is classified as a voltage-controlled memcapacitive (memory capacitive) system. Voltage-controlled memcapacitive systems[37] are described by the equations

$$q(t) = C(x, V, t)V(t) \tag{2}$$

$$\frac{dx}{dt} = f(x, V, t) \tag{3}$$

where $q(t)$ is the charge on the capacitor at time t, $V(t)$ is the applied voltage, C is the memcapacitance, which depends on the state of the system and can vary in time, x is a set of n state variables describing the internal state of the system, and f is a continuous n-dimensional vector function. An important step in the memory device modeling is the identification of specific physical mechanisms[38] responsible for memory response and associated internal state variables. In S8 of theSupporting Information, we present a network model of memory effects in Sr:HfO_2 in which a discretized density of defects plays the role of internal state variables. This model is able to reproduce all properties of the split-up/merging phenomenon as shown in Figure S11 of the Supporting Information.

CONCLUSION

A more detailed look into defect-related mechanisms of a rather new, promising, ferroelectric material was presented. As a simple binary oxide, HfO_2 could serve as a model system to further study the fundamentals of ferroelectricity in a system without complex composition and chemistry. A time-saving and convenient approach harmonic analysis was used to study the temperature and frequency dependence of three phenomena in Sr:HfO_2: (1) wake-up, (2) polarization fatigue, and (3) pinching/depinching of the hysteresis by electric field cycling. The obtained activation energies were in the range of 50−200 meV for wake-up, fatigue, and split-up/merging effect but showed different frequency dependences. Compared to the values obtained for PZT, these energies are nearly 1 order of magnitude lower, which was attributed to the comparably high applied fields for Sr:HfO_2. Also, the much higher number of grain boundaries and corresponding defects per volume compared to the PZT ceramics in other studies should be taken into account. Moreover, the novel analog split-up/merging phenomenon was, to the author's knowledge, reported here for the first time. A modeling approach based on memcapacitive behavior was used to explain the observed phenomena as a result of different local defect concentrations. It was assumed that the observed cycling response is associated with a migration of defects from actively switching domains (at a given cycling field amplitude) to passive ones. Although temperature-dependent studies were only performed for 3.4 cat % Sr, the behavior is similar for other concentrations and other dopant materials. Tuning the kinetics of this effect by appropriate processing, it might be of special interest for multilevel cell memories[39] or smart operating schemes with a rejuvenation of a fatigued P_r by only a few pulses of higher amplitude after a certain amount of stress cycles to prolong the endurance of the memory cell.

EXPERIMENTAL PROCEDURES

Metal-ferroelectric-metal (MFM) stacks were fabricated on a lightly p-doped Si substrate. The TiN bottom electrode and the Sr:HfO_2 dielectric, 10 nm each, were deposited by reactive magnetron sputtering at room temperature and thermal atomic layer deposition (ALD) at 300 °C, respectively. The Sr content of the sample was adjusted by the ratio of HfO_2 and SrO ALD cycles using a $HfCl_4/H_2O$ and a $Sr(^tBu_3Cp)_2/H_2O$ process. The resulting Sr content was determined to be 3.4 cat% (cat% = Sr/[Hf + Sr]) by Rutherford backscattering spectroscopy. The further sample preparation included a reactive magnetron sputtering of the 12 nm TiN top electrodes (TE) at 200 °C and a N_2 anneal for 20 s at 800 °C to crystallize the previously amorphous Sr:HfO_2. Finally, circular contact pads consisting of a 10 nm adhesion layer of Ti and 50 nm Pt were deposited through a shadow mask on top of the samples in an electron beam evaporator. These pads define the MFM capacitor structures subsequently patterned by an SC1 etch to remove the TiN TE. Electrical measurements were performed with a TF Analyzer 3000 with FE-Module (aixACCT Systems). Harmonic analysis[20,21] was applied to study the wake-up and the split-up/merging effect. Phase jumps in seventh and ninth harmonic were used as an indicator for a transition between a pinched and a depinched hysteresis shape. In contrast to the direct measurement with lock-in technique presented in refs 20 and 21, here the fatigue measurement environment of the TF Analyzer 3000 was used. Within this environment, rectangular stress cycles and triangular measurement cycles were applied during the dynamic hysteresis measurements to extract a $P-E$ hysteresis 3 times per 10 stress cycles. Afterward, the data was subjected to a Fourier series expansion to obtain amplitude and phase values of the respective harmonics and to plot this data against the number of field cycles as shown in Figure 3a. This procedure was repeated for different temperatures to plot the time of the phase jump versus inverse temperature to extract the activation energy of the seventh and ninth harmonic. For the fatigue effect, the approach was different. Here, the onset of fatigue was linked to a point in time when P_r started decreasing and not to phase jumps in any harmonic.

ASSOCIATED CONTENT

Supporting Information

Sample preparation, measurement setup. Harmonic analysis and a comparison to the Preisach model. Polarization hystereses and transient current graphs for different temperatures. Arrhenius-plots for all extracted activation energies. Details on the memcapacitive network model and its results. This material is available free of charge via the Internet at http://pubs.acs.org.

AUTHOR INFORMATION

Corresponding Author

*E-mail: tony.schenk@namlab.com.

Notes

The authors declare no competing financial interest.

■ ACKNOWLEDGMENTS

Bernd Reichenberg from aixACCT Systems is gratefully acknowledged for the valuable discussions and rapid development of the upgrade necessary to perform the measurements for this work. Moreover, the German Research Foundation (Deutsche Forschungsgemeinschaft) is acknowledged for funding this research within the project Inferox (MI 1247/11-1).

■ REFERENCES

(1) Böscke, T. S.; Müller, J.; Bräuhaus, D.; Schröder, U.; Böttger, U. Ferroelectricity in Hafnium Oxide Thin Films. *Appl. Phys. Lett.* **2011**, *99*, 102903.

(2) Clima, S.; Wouters, D. J.; Adelmann, C.; Schenk, T.; Schroeder, U.; Jurczak, M.; Pourtois, G. Identification of the Ferroelectric Switching Process and Dopant-Dependent Switching Properties in Orthorhombic HfO_2: A First Principles Insight. *Appl. Phys. Lett.* **2014**, *104*, 092906.

(3) Huan, T. D.; Sharma, V.; Rossetti, G. A., Jr.; Ramprasad, R. Pathways Towards Ferroelectricity in Hafnia. *Phys. Rev. B* **2014**, *90*, 064111.

(4) Bennett, J. W.; Garrity, K. F.; Rabe, K. M.; Vanderbilt, D. Orthorhombic ABC Semiconductors as Antiferroelectrics. *Phys. Rev. Lett.* **2013**, *110*, 017603.

(5) Reyes-Lillo, S. E.; Garrity, K. F.; Rabe, K. M. Antiferroelectricity in Thin Film ZrO_2 from First Principles. *Phys. Rev. B* **2014**, *90*, 140103(R).

(6) Park, M. H.; Kim, H. J.; Kim, Y. J.; Lee, W.; Kim, H. K.; Hwang, C. S. Effect of Forming Gas Annealing on the Ferroelectric Properties of $Hf_{0.5}Zr_{0.5}O_2$ Thin Films with and without Pt Electrodes. *Appl. Phys. Lett.* **2013**, *102*, 112914.

(7) Lomenzo, P. D.; Zhao, P.; Takmeel, Q.; Moghaddam, S.; Nishida, T.; Nelson, M.; Fancher, C. M.; Grimley, E. D.; Sang, X.; LeBeau, J. M.; Jones, J. L. Ferroelectric Phenomena in Si-Doped HfO_2 Thin Films with TiN and Ir Electrodes. *J. Vac. Sci. Technol., B: Nanotechnol. Microelectron.: Mater., Process., Meas., Phenom.* **2014**, *32*, 03D123.

(8) Park, M. H.; Kim, H. J.; Kim, Y. J.; Moon, T.; Kim, K. D.; Hwang, C. S. Thin $Hf_xZr_{1-x}O_2$ Films: A New Lead-Free System for Electrostatic Supercapacitors with Large Energy Storage Density and Robust Thermal Stability. *Adv. Energy Mater.* **2014**, *1400610*, 1−7.

(9) Luo, X.; Zhou, W.; Ushakov, S. V.; Navrotsky, A.; Demkov, A. A. Monoclinic to Tetragonal Transformations in Hafnia and Zirconia: A Combined Calorimetric and Density Functional Study. *Phys. Rev. B* **2009**, *80*, 134119.

(10) Bohr, M.; Chau, R.; Ghani, T.; Mistry, K. The High-k Solution. *IEEE Spectrum* **2007**, *44*, 29−35.

(11) International Technology Roadmap for Semiconductors − Emerging Research Devices. http://www.itrs.net/Links/2013ITRS/2013Chapters/2013ERD.pdf (accessed Sept 28, 2014).

(12) Müller, J.; Yurchuk, E.; Schlösser, T.; Paul, J.; Hoffmann, R.; Mueller, S.; Martin, D.; Slesazeck, S.; Polakowski, P.; Sundqvist, J.; Czernohorsky, M.; Seidel, K.; Kücher, P.; Boschke, R.; Trentzsch, M.; Gebauer, K.; Schröder, U.; Mikolajick, T. Ferroelectricity in HfO_2 Enables Nonvolatile Data Storage in 28 nm HKMG. *Symposium on VLSI Technology (VLSIT)*, Honolulu, HI, June 12−14, 2012; IEEE: Piscataway, NJ, 2012; pp 25−26.

(13) Schenk, T.; Mueller, S.; Schroeder, U.; Materlik, R.; Kersch, A.; Popovici, M.; Adelmann, C.; Van Elshocht, S.; Mikolajick, T. Strontium Doped Hafnium Oxide Thin Films: Wide Process Window for Ferroelectric Memories. *ESSDERC 2013, Proc. Eur. Solid-State Device Res. Conf., 43rd* **2013**, 260−263.

(14) Carl, K.; Hardtl, K. H. Electrical After-Effects in $Pb(Ti, Zr)O_3$ Ceramics. *Ferroelectrics* **1977**, *17*, 473−486.

(15) Schenk, T.; Yurchuk, E.; Müller, S.; Schröder, U.; Starschich, S.; Böttger, U.; Mikolajick, T. Physical Roots for the Deformation of Ferroelectric Hystereses. *Appl. Phys. Rev.* accepted for publication.

(16) Olsen, T.; Schroder, U.; Muller, S.; Krause, A.; Martin, D.; Singh, A.; Müller, J.; Geidel, M.; Mikolajick, T. Co-Sputtering Yttrium into Hafnium Oxide Thin Films to Produce Ferroelectric Properties. *Appl. Phys. Lett.* **2012**, *101*, 082905.

(17) Zhou, D.; Xu, J.; Li, Q.; Guan, Y.; Cao, F.; Dong, X.; Müller, J.; Schenk, T.; Schröder, U. Wake-up Effects in Si-Doped Hafnium Oxide Ferroelectric Thin Films. *Appl. Phys. Lett.* **2013**, *103*, 192904.

(18) Schroeder, U.; Yurchuk, E.; Müller, J.; Martin, D.; Schenk, T.; Polakowski, P.; Adelmann, C.; Popovici, M.; Kalinin, S. V.; Mikolajick, T. Impact of Different Dopants on the Switching Properties of Ferroelectric Hafniumoxide. *Jpn. J. Appl. Phys.* **2014**, *53*, 08LE02.

(19) Menou, N.; Muller, C.; Baturin, I. S.; Shur, V. Y.; Hodeau, J.-L. Polarization Fatigue in $PbZr_{0.45}Ti_{0.55}O_3$-Based Capacitors Studied from High Resolution Synchrotron X-Ray Diffraction. *J. Appl. Phys.* **2005**, *97*, 064108.

(20) Morozov, M. I. Softening and Hardening Transitions in Ferroelectric $Pb(Zr,Ti)O_3$ Ceramics. PhD thesis, EPFL − Swiss Federal Institute of Technology, Lausanne, Nov 2005.

(21) Morozov, M. I.; Damjanovic, D. Hardening-Softening Transition in Fe-Doped $Pb(Zr,Ti)O_3$ Ceramics and Evolution of the Third Harmonic of the Polarization Response. *J. Appl. Phys.* **2008**, *104*, 034107.

(22) Preisach, F. Über die Magnetische Nachwirkung. *Z. Physik* **1935**, *94*, 277−302.

(23) Scott, J. F. *Ferroelectric Memories*; Springer-Verlag: Berlin, 2000.

(24) Robels, U.; Schneider-Störmann, L.; Arlt, G. Dielectric Aging and its Temperature Dependence in Ferroelectric Ceramics. *Ferroelectrics* **1995**, *168*, 301−311.

(25) Warren, W. L.; Vanheusden, K.; Dimos, D.; Pike, G. E.; Tuttle, B. A. Oxygen Vacancy Motion in Perovskite Oxides. *J. Am. Ceram. Soc.* **1996**, *79*, 536−538.

(26) Goux, L.; Czarnecki, P.; Chen, Y. Y.; Pantisano, L.; Wang, X. P.; Degraeve, R.; Govoreanu, B.; Jurczak, M.; Wouters, D. J.; Altimime, L. Evidences of Oxygen-Mediated Resistive-Switching Mechanism in TiN \HfO_2\Pt Cells. *Appl. Phys. Lett.* **2010**, *97*, 243509.

(27) Tucker, M. C. Progress in Metal-Supported Solid Oxide Fuel Cells: A Review. *J. Power Sources* **2010**, *195*, 4570−4582.

(28) Laguna-Bercero, M. A. Recent Advances in High Temperature Electrolysis Using Solid Oxide Fuel Cells: A Review. *J. Power Sources* **2012**, *203*, 4−16.

(29) Kharton, V. V.; Yaremchenko, A. A.; Naumovich, E. N.; Marques, F. M. B. Research on the Electrochemistry of Oxygen Ion Conductors in the Former Soviet Union III. HfO_2-, CeO_2- and ThO_2-Based Oxides. *J. Solid State Electrochem.* **2000**, *4*, 243−266.

(30) Kharton, V. V.; Naumovich, E. N.; Vecher, A. A. Research on the Electrochemistry of Oxygen Ion Conductors in the Former Soviet Union I. ZrO_2-Based Ceramic Materials. *J. Solid State Electrochem.* **1999**, *3*, 61−81.

(31) Capron, N.; Broqvist, P.; Pasquarello, A. Migration of oxygen vacancy in HfO_2 and across the HfO_2/SiO_2 interface: A first-principles investigation. *Appl. Phys. Lett.* **2007**, *91*, 192905.

(32) Martin, D.; Müller, J.; Schenk, T.; Arruda, T. M.; Kumar, A.; Strelcov, E.; Yurchuk, E.; Müller, S.; Pohl, D.; Kersch, A.; Schröder, U.; Kalinin, S. V.; Mikolajick, T. Ferroelectricity in Si-Doped HfO_2 Revealed: A Binary Lead-Free Ferroelectric. *Adv. Mater.* **2014**, DOI: 10.1002/adma.201403115.

(33) Knebel, S.; Kupke, S.; Schroeder, U.; Slesazeck, S.; Mikolajick, T.; Agaiby, R.; Trentzsch, M. Influence of Frequency Dependent Time to Breakdown on High-k/Metal Gate Reliability. *IEEE Trans. Electron Devices* **2013**, *60*, 2368−2371.

(34) Bersuker, G.; Heh, D.; Young, C.; Park, H.; Khanal, P.; Larcher, L.; Padovani, A.; Lenahan, P.; Ryan, J.; Lee, B. H.; Tseng, H.; Jammy, R. Breakdown in the Metal/High-k Gate Stack: Identifying the 'Weak Link' in the Multilayer Dielectric. *Proc. IEEE Int. Electron Devices Meet.* **2008**, 1−4.

(35) Tagantsev, A. K.; Stolichnov, I.; Colla, E. L.; Setter, N. Polarization Fatigue in Ferroelectric Films: Basic Experimental Findings, Phenomenological Scenarios, and Microscopic Features. *J. Appl. Phys.* **2001**, *90*, 1387.

(36) Di Ventra, M.; Pershin, Y. V. Memory Materials: A Unifying Description. *Mater. Today* **2011**, *14*, 584−591.

(37) Di Ventra, M.; Pershin, Y. V.; Chua, L. O. Circuit Elements With Memory: Memristors, Memcapacitors, and Meminductors. *Proc. IEEE* **2009**, *97*, 1717−1724.
(38) Pershin, Y. V.; Di Ventra, M. Memory Effects in Complex Materials and Nanoscale Systems. *Adv. Phys.* **2011**, *60*, 145−227.
(39) Bauer, M.; Alexis, R.; Atwood, G.; Baltar, B.; Fazio, A.; Frary, K.; Hensel, M.; Ishac, M.; Javanifard, J.; Landgraf, M.; Leak, D.; Loe, K.; Mills, D.; Ruby, P.; Rozman, R.; Sweha, S.; Talreja, S.; Wojciechowski, K. A Multilevel-Cell 32 Mb Flash Memory. *IEEE Int. Solid-State Circuits Conference (ISSCC), Dig. Tech. Pap.* **1995**, 132−133.